Intracrine testosterone activation in human pancreatic β cells stimulates insulin secretion.

Weiwei Xu, Lina Schiffer, M.M. Fahd Qadir, Yanqing Zhang, Paula Mota De Sa, Brian G Keevil, Hongju Wu, Wiebke Arlt, Franck Mauvais-Jarvis

Supplementary File

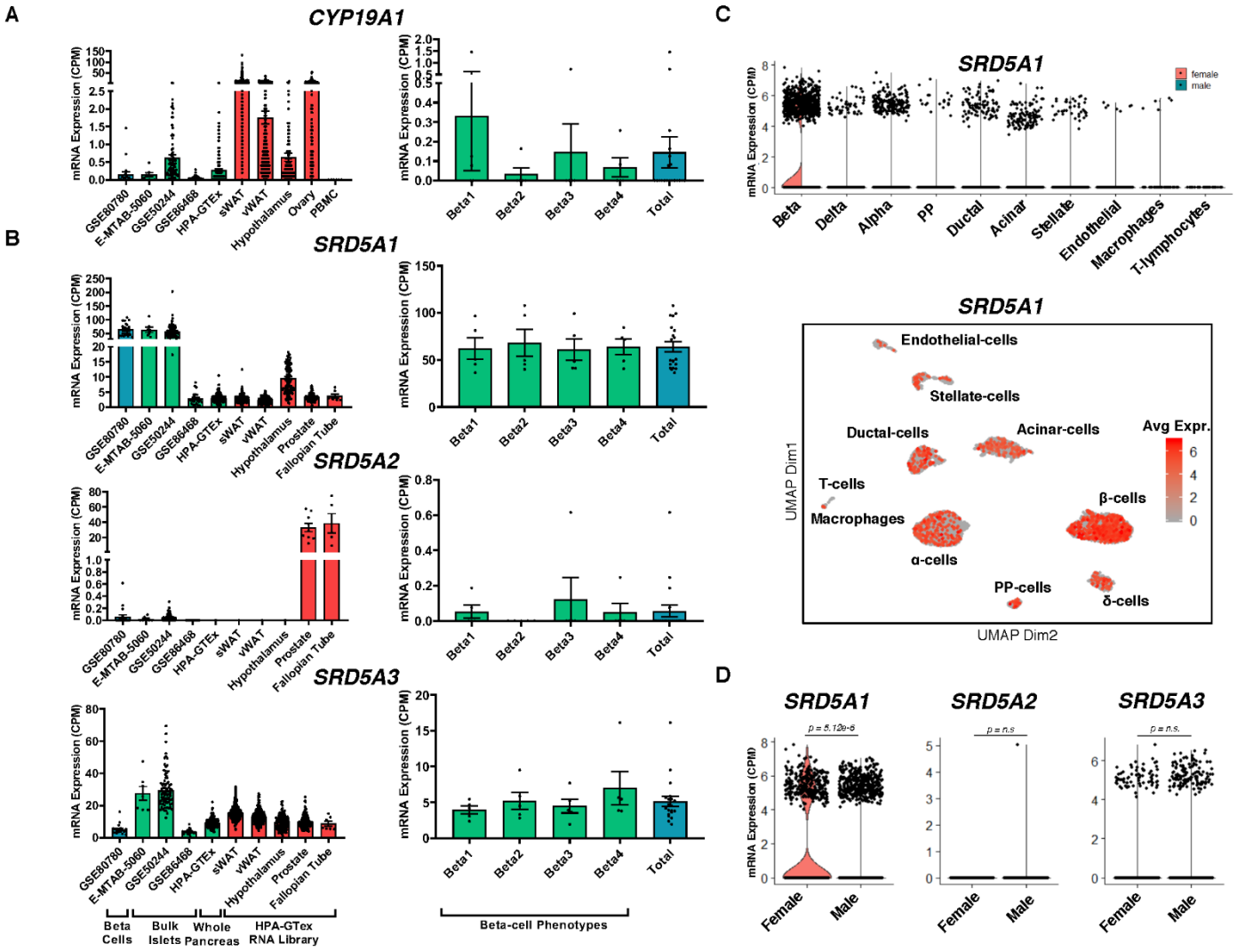

Supplementary Figure 1. Human pancreatic β cells expression CYP19A1 and SRD5A1-3 in RNA-seq datasets. Normalized mRNA expression of **(A)** CYP19A1 and **(B)** SRD5A1-3. Left panels represent scatter plots with mean ± SD of mRNA expression (counts per million) from FACS sorted β cells (GSE80780), bulk islets (E-MTAB-5060, GSE50244 and GSE86468), whole pancreas (HPA-GTEx) and control tissues (sWAT: subcutaneous white adipose tissue, vWAT: visceral white adipose tissue, hypothalamus, prostate, ovary, PBMCs: peripheral blood mononuclear cells, and fallopian tubes). Right panels represent scatter plot with mean ± SD of mRNA expression (counts per million) from FACS sorted β cells from 4 different phenotypes as described in methods, and all 4 β cell phenotypes combined (derived from GSE80780 denoted in the right panel). **(C)** Normalized mRNA expression of SRD5A1 in a single-cell mRNA expression atlas of pancreatic islets cells (GSE84133). Top panel represents violin plots showing the distribution of data points and probability density of their overall expression. The plots are split in two halves, the left half denoting female while the right half denoting male expression levels. Bottom panel represents a non-linear multidimensional uniform maximal projection (UMAP) map showing expression distribution of SRD5A1 across different cell types in pancreatic islets. **(D)** Normalized mRNA expression of SRD5A1-3 in human pancreatic β cells derived from a single cell mRNA-Seq expression atlas of pancreatic islets (GSE84133). Data are represented as violin plots showing distribution of data points and the probability density of their overall expression. Information on donor numbers is provided in the methods.

Methods for Supplementary Figure 1.

Supplemental data files containing count information was downloaded from publicly available datasets (data were collectively accessed on: 4/27/2020). A description of the raw datafiles and their relevant citations is shown in the table below:

Dataset Identifier	Dataset Characteristics	Dataset link	Citation	Sample Number
GSE80780	FACS sorted human β cell subtype bulk RNAseq	https://www.ncbi.nlm.nih.gov/geo/query/acc.cgi?acc=GSE80780	[1]	*n* = 5
E-MTAB-5060	Human Islet bulk RNAseq	https://www.ebi.ac.uk/arrayexpress/experiments/E-MTAB-5060/	[2]	*n* = 5
GSE50244	Human Islet bulk RNAseq	https://www.ncbi.nlm.nih.gov/geo/query/acc.cgi?acc=GSE50244	[3-7]	*n* = 89
GSE86468	Human Islet bulk RNAseq	https://www.ncbi.nlm.nih.gov/geo/query/acc.cgi?acc=GSE86468	[8]	*n* = 24
HPA-GTEx	Human tissue bulk RNAseq	https://www.proteinatlas.org/ENSG00000137869-CYP19A1/tissue https://www.proteinatlas.org/ENSG00000145545-SRD5A1/tissue https://www.proteinatlas.org/ENSG00000277893-SRD5A2/tissue https://www.proteinatlas.org/ENSG00000128039-SRD5A3	[9-11]	*n* = 7-442
GSE84133/ GSM2230757/ GSM2230758/ GSM2230759/ GSM2230760	Human islet single cell RNAseq	https://www.ncbi.nlm.nih.gov/geo/query/acc.cgi?acc=GSE84133 https://www.ncbi.nlm.nih.gov/geo/query/acc.cgi?acc=GSM2230757 https://www.ncbi.nlm.nih.gov/geo/query/acc.cgi?acc=GSM2230758 https://www.ncbi.nlm.nih.gov/geo/query/acc.cgi?acc=GSM2230759 https://www.ncbi.nlm.nih.gov/geo/query/acc.cgi?acc=GSM2230760	[12]	*n* = 4

In case of GSE80780, we plotted the bulk RNAseq expression profiles of 4 distinct FACS sorted β cell subtypes as identified and described in[1]. Once downloaded, raw mRNA count files were

converted into counts per million (CPM) using either DESeq2's[13] normalization pipeline (bulk RNAseq data) or Seurat v3.1.4[14,15] (single cell RNAseq data) normalization and integration pipeline for CPM using the following R function:

```
(GSE84133.integrated <- NormalizeData(GSE84133.integrated, scale.factor = 1e6, assay = 'RNA',
verbose = TRUE
```

In case of the GSE84133, a Wilcoxon *t*-test was run to evaluate the significance for the mRNA expression between males and females. The following code in R was used to perform this function:

```
# Extract expression matrix for all beta cells

betacells <- subset(GSE84133.integrated, idents = c("1"))

# Set cell identity to sample identity

Idents(object = betacells) <- betacells@meta.data$sample

# Find if SRD5A1-3 genes are differentially expressed

beta.integrated.markers <- FindAllMarkers(object = betacells, slot = 'data', test.use = 'wilcox')
```

Data was then plotted using either Seurat's built in VlnPlot function or using GraphPad Prism v8.

References

1 Dorrell, C. *et al.* Human islets contain four distinct subtypes of β cells. *Nature communications* **7**, 11756, doi:10.1038/ncomms11756 (2016).

2 Segerstolpe, Å. *et al.* Single-Cell Transcriptome Profiling of Human Pancreatic Islets in Health and Type 2 Diabetes. *Cell metabolism* **24**, 593-607, doi:10.1016/j.cmet.2016.08.020 (2016).

3 Zhou, Y. *et al.* TCF7L2 is a master regulator of insulin production and processing. *Human molecular genetics* **23**, 6419-6431, doi:10.1093/hmg/ddu359 (2014).

4 Fadista, J. *et al.* Global genomic and transcriptomic analysis of human pancreatic islets reveals novel genes influencing glucose metabolism. *Proceedings of the National Academy of Sciences of the United States of America* **111**, 13924-13929, doi:10.1073/pnas.1402665111 (2014).

5 Taneera, J. *et al.* Identification of novel genes for glucose metabolism based upon expression pattern in human islets and effect on insulin secretion and glycemia. *Human molecular genetics* **24**, 1945-1955, doi:10.1093/hmg/ddu610 (2015).

6 Malenczyk, K. *et al.* A TRPV1-to-secretagogin regulatory axis controls pancreatic β-cell survival by modulating protein turnover. *The EMBO journal* **36**, 2107-2125, doi:10.15252/embj.201695347 (2017).

7 Taneera, J. *et al.* Orphan G-protein coupled receptor 183 (GPR183) potentiates insulin secretion and prevents glucotoxicity-induced β-cell dysfunction. *Molecular and cellular endocrinology* **499**, 110592, doi:10.1016/j.mce.2019.110592 (2020).

8 Lawlor, N. *et al.* Single-cell transcriptomes identify human islet cell signatures and reveal cell-type-specific expression changes in type 2 diabetes. *Genome research* **27**, 208-222, doi:10.1101/gr.212720.116 (2017).

9 Thul, P. J. *et al.* A subcellular map of the human proteome. *Science (New York, N.Y.)* **356**, doi:10.1126/science.aal3321 (2017).

10 Uhlén, M. *et al.* Proteomics. Tissue-based map of the human proteome. *Science (New York, N.Y.)* **347**, 1260419, doi:10.1126/science.1260419 (2015).

11 Uhlen, M. *et al.* Towards a knowledge-based Human Protein Atlas. *Nature biotechnology* **28**, 1248-1250, doi:10.1038/nbt1210-1248 (2010).

12 Baron, M. *et al.* A Single-Cell Transcriptomic Map of the Human and Mouse Pancreas Reveals Inter- and Intra-cell Population Structure. *Cell systems* **3**, 346-360.e344, doi:10.1016/j.cels.2016.08.011 (2016).
13 Love, M. I., Huber, W. & Anders, S. Moderated estimation of fold change and dispersion for RNA-seq data with DESeq2. *Genome Biology* **15**, 550, doi:10.1186/s13059-014-0550-8 (2014).
14 Butler, A., Hoffman, P., Smibert, P., Papalexi, E. & Satija, R. Integrating single-cell transcriptomic data across different conditions, technologies, and species. *Nature biotechnology* **36**, 411-420, doi:10.1038/nbt.4096 (2018).
15 Stuart, T. *et al.* Comprehensive Integration of Single-Cell Data. *Cell* **177**, 1888-1902.e1821, doi:10.1016/j.cell.2019.05.031 (2019).

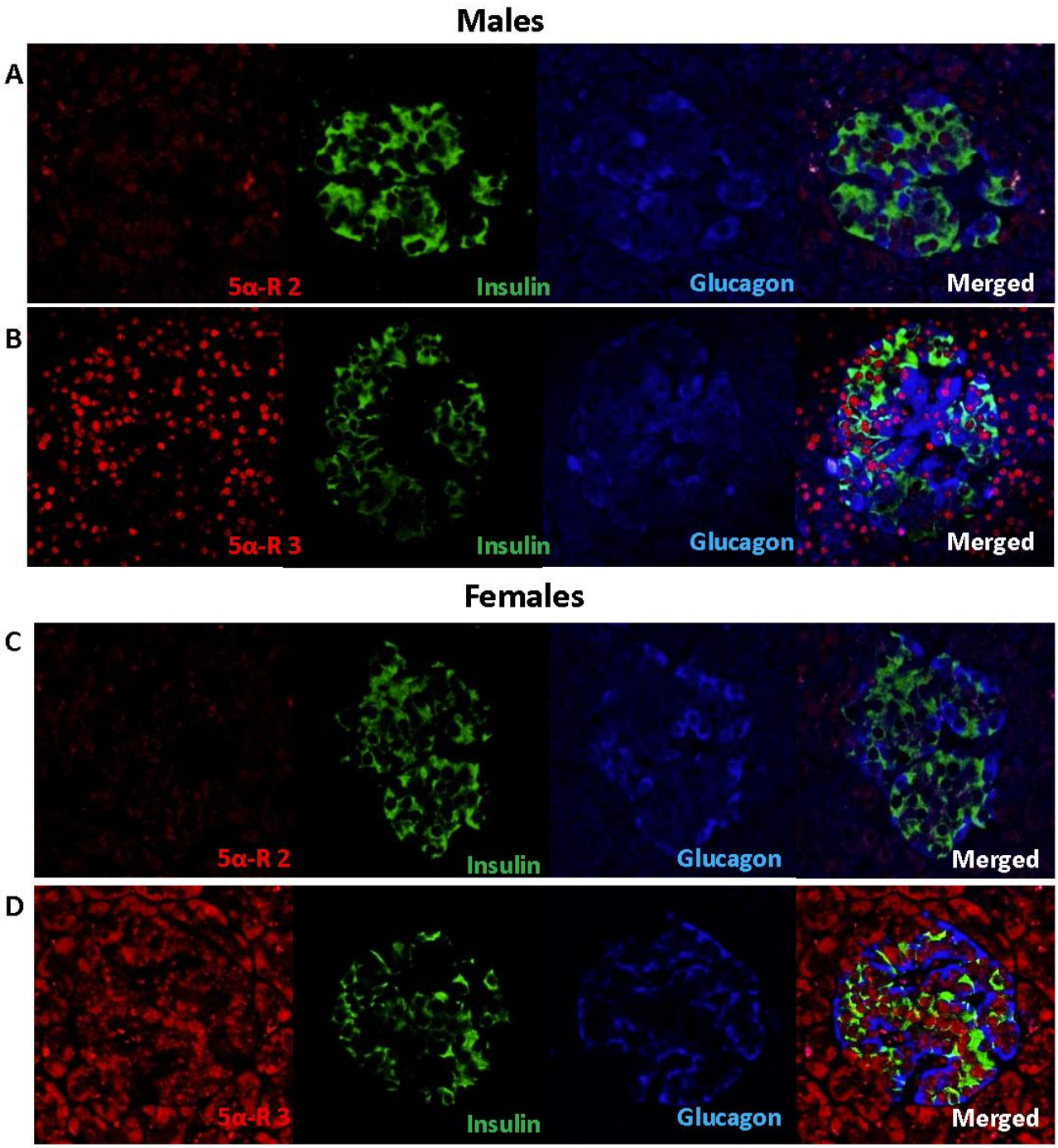

Supplementary Figure 2. Expression of SRD5A2 and SRD5A3 in human islets. IHC staining of SRD5A1 and SRD5A3 (red), insulin (green) and glucagon (blue) in pancreas sections from male and female non-diabetic human donors. Representative images are shown.

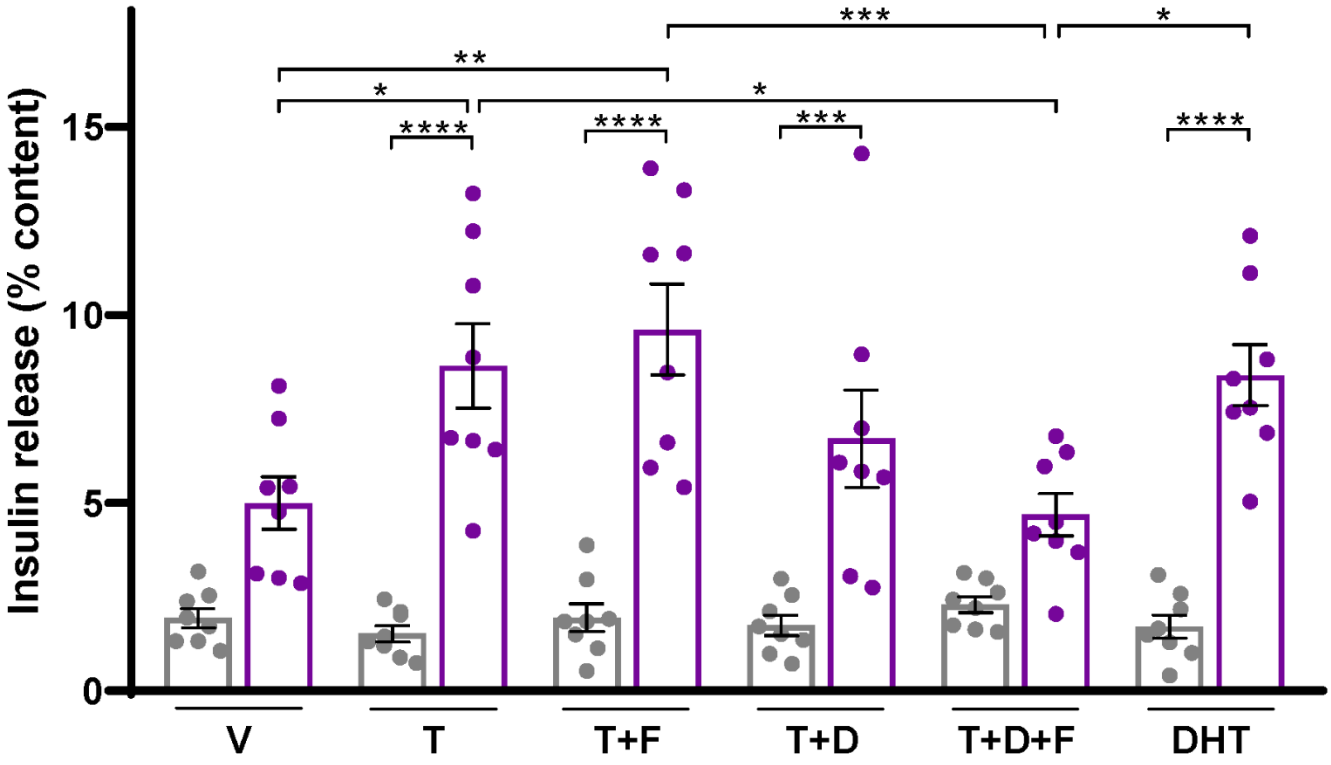

Supplementary Figure 3. Inhibition of SRD5A1, not SRD5A2 or 3 prevents testosterone-induced amplification of GSIS. GSIS measured in static incubation in human islets treated with vehicle, T (10nM), finasteride (F, 100nM) or dutasteride (D, 100nM), or both D +F, and DHT (10nM). The mean ± SEM and scatter plot of technical quadriplicates from one male and one female donors are shown. *P < 0.05, **P < 0.01, ***P < 0.001.

Donor characteristics are as follows

HP-20066-01:

1. Non-diabetic
2. 60 yo
3. Female
4. Caucasian
5. 61” height
6. 139lbs weight
7. 25.8 BMI
8. Stroke COD
9. 5.1% HbA1c

HP-20071-01:

1. Non-diabetic
2. 42 yo
3. Male
4. Caucasian
5. 75” height
6. 224 lbs weight
7. 28.1 BMI
8. Head trauma COD
9. 4.9% HbA1c

Supplementary method for UHPLC-MS/MS

Both the assay for the androgen panel and the assay for E2 were validated according to industry standard (Guidance for industry. Bioanalytical method validation. US Department of Health and Human Services. Food and Drug Administration, Centre for Drug Evaluation and Research (CDER) and Centre for Veterinary Medicine (CVM), 2018).

For the androgen assay multiplexing testosterone, 5α-dihydrotestosterone (DHT), androstenedione (A4), 5α-androstanedione (A-dione) and 5α-androsterone (An), the bias between nominal and measured concentrations (representing accuracy) assessed at three different concentrations was between +12 and -12% for all analytes. The coefficient of variation (%CV) for either the intra- or inter-assay imprecision, assessed for pooled biological samples and for matrix-matched samples, spiked at three different concentrations and did not exceed 8% for all analytes except androstenedione, for which it was <22%. Matrix effects were within ± 20% across 6 samples for all analytes. Limits of quantifications were 0.24 nM for T, 2.8 nM for A4, 0.24 nM for DHT, 0.8 nM Adione and 0.8 nM for An.

For the E2 assay, the bias between nominal and measured concentrations (representing accuracy) was no greater than 8% for all 5 concentrations assessed. The coefficient of variation (%CV) did not exceed 7% for either the intra- or inter-assay imprecision at 5 different concentrations and for pooled biological samples. The assay had a mean recovery of 113% for three different concentrations assessed. The mean matrix effect across 6 samples and 3 concentrations was -12%. The limit of quantification was 10 pM and the limit of detection was 5pM. Comparison using patient serum samples against a previously published version of this assay (Owen LJ et al., Ann Clin Biochem 2014;51:360-367) showed a difference of -0.11%. The assay has been accredited against ISO 15189.

Note that we report only concentrations that are above the lower limit of quantification (LLOQ), which is the lowest concentration that can still be reliably quantified with precision (CV <20%) and accuracy (bias within +/-20%). This is assessed during assay validation by measuring replicate samples of low concentrations.

We have applied our UHPLC-MS/MS assay in previous studies investigating steroid metabolism in other human peripheral tissues ex-vivo similar to the investigations we present here for human pancreatic islets. Our previous studies using this assay included ovarian follicles (Lebbe M et al., Endocrinology 2017, 158:1474-1485), subcutaneous adipose tissue (Markey K et al., Brain Communications 2020, 2(10), fcz050, https://doi.org/10.1093/braincomms/fcz050) and adrenal and gonadal tissue (Reisch N, Taylor AE et al., Proc Natl Acad Sci U S A. 2019 Oct 29;116(44):22294-22299). This information is provided in the revised Supplementary method section.